Non-saturation of the defect moment of goethite and fine-grained hematite up to 57 Teslas

Pierre Rochette, Pierre-Etienne Mathé, Lionel Esteban, Harison Rakoto, Jean-Luc Bouchez, Qingsong Liu, José Torrent

Non-saturation of the defect moment of goethite and fine-grained hematite up to 57 Teslas

Pierre Rochette,[1] Pierre-Etienne Mathé,[1] Lionel Esteban,[2] Harison Rakoto,[3] Jean-Luc Bouchez,[2] Qingsong Liu,[4] and José Torrent[5]

Received 26 July 2005; revised 27 September 2005; accepted 11 October 2005; published 23 November 2005.

[1] Defect moment of antiferromagnets yields the highest remanent coercivity observed among minerals, and previous studies have been unable to reach saturation of isothermal remanent magnetization (IRM) in some goethite and hematite, even up to 20 Teslas, using resistive Bitter magnets. To go further, acquisition of IRM at room temperature has been monitored on various natural and synthetic goethite and hematite samples in pulsed magnetic fields up to 57 Teslas. ''Coarse'' hematite is saturated around 5 T, and low unblocking temperature (T_B, i.e. with low crystallinity or Al substitution) goethites saturate around 20 T. Higher T_B goethites and a Mn-bearing fine-grained hematite are still not saturated even at 57 T, with only 2 to 10 percent of the maximum IRM acquired in 3 T. Half acquisition fields are mostly above 10 T. This indicates that usual rock magnetic techniques strongly underestimate the contribution of such minerals to remanence. IRM acquisition is strongly irreversible: in some samples a 57 T backfield is unable to erase a previous 38 T IRM. A field induced defect diffusion model is put forward to account for remanence acquisition in these materials. **Citation:** Rochette, P., P.-E. Mathé, L. Esteban, H. Rakoto, J.-L. Bouchez, Q. Liu, and J. Torrent (2005), Non-saturation of the defect moment of goethite and fine-grained hematite up to 57 Teslas, *Geophys. Res. Lett.*, *32*, L22309, doi:10.1029/2005GL024196.

1. Introduction

[2] The antiferromagnetic minerals goethite (α–FeOOH) and hematite (α–Fe_2O_3) are known to carry a defect moment along the antiferromagnetic axis [*Dunlop*, 1971; *Özdemir and Dunlop*, 1996]. This moment is responsible for the remanent magnetization in many natural materials on Earth and Mars surfaces [*Schwertmann and Taylor*, 1989; *Chevrier et al.*, 2004]. Both minerals exhibit spin-flop transitions at high magnetic field [*Coey et al.*, 1995; *Van San et al.*, 2004]. Hematite also exhibits an intrinsic weak ferromagnetism superimposed upon the defect moment [*Dunlop*, 1971]. Room temperature isothermal remanent magnetization (RT IRM) of these two minerals is very hard and magnetic fields available in most rock magnetic laboratories (1–3 T range) are unable to approach saturation. The use of cryogenic magnets up to 7 T [*Maher et al.*, 2004], pulse fields up to 7 or 9 T [*France and Oldfield*, 2000; *Walden et al.*, 2000], and Bitter magnets up to 15–20 T [*Dekkers*, 1989; *Rochette and Fillion*, 1989], has proved to be insufficient to reach saturation in both minerals. In this study, we have monitored the RT IRM acquisition of selected samples of synthetic and natural goethite and hematite in very high pulse fields up to 57 T and report here that most samples are still far from saturation.

2. Samples

[3] Three different pure goethite powders were pressed in 6 mm diameter pellets of 32 to 360 mg each. Samples CB22 and 39/80 were synthesized from Fe salt solutions [*Torrent et al.*, 1987, 1990]. They are similar to the samples showing non-saturation at 15 T [*Rochette and Fillion*, 1989], the crystallite size of which is in the 0.1-1 μm range. GT is a natural hydrothermal fibrous goethite from Tarn (S France) that has been manually powdered (at <50 μm). Table 1 provides their X-ray diffraction parameters as well as the maximum unblocking temperature of remanence T_B, found close to their Néel point [*Rochette and Fillion*, 1989; *Coey et al.*, 1995; *Özdemir and Dunlop*, 1996; *Liu et al.*, 2004]. Chemical analysis (using ICP-AES) of GT demonstrates only 0.42 wt.% of impurities, including 0.16% H_2O, 0.12% SiO_2, and Ca, K, Ga for the >100 ppm elements, at 500, 400 and 220 ppm, respectively. Ga is likely to be structural while Si, Ca, K probably correspond to mineral inclusions. Three cylindrical rock samples (12 mm diameter, 5 mm height) were also selected from previous paleomagnetic and rock magnetic studies. RD is a goethite-bearing Jurassic limestone (from Cote d'Or, E France) with maximum T_B of 360 K, bearing a geologically stable natural remanence [*Dekkers and Rochette*, 1992]. RR is a Permian volcanic rock (the Reyran rhyolite) from Esterel (SE France) with maximum T_B of 660°C [*Vlag et al.*, 1997] typical of high temperature well crystallized hematite with minor Ti substitution, thus likely with dominant weak ferromagnetism. Finally TO is a Cretaceous iron-rich deep-sea sediment (''umber'' from the Oman ophiolite) bearing low temperature very fine hematite, likely substituted with Mn, with maximum T_B of 640°C [*Thomas et al.*, 1988]. The same rock exhibited non-saturation up to 15 Tesla [*Rochette and Fillion*, 1989], indicating, together with the mode of formation, a dominant defect moment. Both RR and TO exhibit a stable primary natural magnetization. Chemical

[1]CEREGE University of Aix-Marseille 3, Aix en Provence, France.
[2]Laboratoire des Mécanismes de Transferts en Géologie, Université de Toulouse, Toulouse, France.
[3]Laboratoire National des Champs Magnétiques Pulsés, Toulouse, France.
[4]Institute of Geophysics and Planetary Physics, University of California, Santa Cruz, California, USA.
[5]Departamento de Ciencias y Recursos Agrícolas y Forestales, Universidad de Córdoba, Córdoba, Spain.

0094-8276/05/2005GL024196

Table 1. Characteristics of the Studied Goethite Powders[a]

	Tbmax, K	RT IRM, mAm^2/kg	$B_{1/2}$, T	A, Å	B, Å	C, Å	MCDa, Å	MCDb, Å
CB22	355	19.9	11	4.615	9.957	3.025	110(47)	244(91)
39/80	380	15	13	4.612	9.956	3.022	293(96)	n.d.
GT	410	7.6	16	4.607	9.962	3.023	537(61)	675(21)

[a]Maximum unblocking temperature was determined using a Micromag VSM, with 2.5 K heating steps (i.e., with a ±5 K uncertainty). Half acquisition field is derived from Figure 1a. Unit cell parameters were obtained from Rietveld refinement of XRD patterns performed on a Philips PW3710 (Co-$K\alpha$, working tension and current intensity respectively 35 kV and 30 mA). Mean coherence lengths along [100] and [010], MCD_a and MCD_b, were calculated using Scherrer formula [*Klug and Alexander*, 1974] as the mean of 110, 120, 130, 111,140 and 020,021 reflections when present, respectively.

analyses give respectively 2.7(0.1), 2.2(0.1) and 16.4(0.6) wt.% $Fe_2O_3(TiO_2)$ for RD, RR and TO, respectively. Mn concentration is 7.6% for TO and negligible for RD and RR.

3. Methods

[4] IRM acquisition, starting from initial state showing negligible remanence, was obtained with pulsed fields, first up to 3 T in CEREGE (using the MMPM9 magnetizer from Magnetic Measurements ltd.), and then from 3.9 to 57 T in the Laboratoire National des Champs Magnétiques Pulsés (LNCMP Toulouse). The two magnets used (maximum fields 40 and 60 T) allow an access of 20 mm diameter and the relative field homogeneity is better than 10^{-3} in the sample zone. Pulse duration is 300 ms and any oscillation toward negative field at the end of the pulse is excluded by the discharge circuit design. Actual maximum fields were 5-15% below nominal values for security reasons. All experiments were conducted at 290 K using a cryostat. Measurement proceeded in two different batches (10 mm diameter rock cylinders and powder pellets of 6 mm diameter), keeping acquisition field along the cylinder axis. A first set of measurements was made using a 40 T magnet, and a second set (one week later) using a 60 T magnet. Subsequently (within 48 hours or two weeks of the acquisition experiment for the 40 and 60 T magnets, respectively), back-field IRM curves were obtained in CEREGE using pulsed fields up to 9 T (small coil of the MMPM9 instrument). Remanence measurements were performed using a JR5A spinner (Agico) installed near the coil, to allow measurements about 5 minutes after field application, while subsequent back-field measurements were performed using a 2G DC SQUID 3 axis magnetometer. Sensitivities are respectively 10^{-10} and 10^{-12} Am^2.

4. Results

[5] Figure 1a shows for the three goethite powders a very limited IRM acquisition below 5 T and a steady increase toward saturation, reached near 30 T for CB22. Samples 39/80 and GT are far from being saturated at 34 T. Half acquisition field of the 34 T IRM is 11, 13, 16 T for CB22, 39/80 and GT, respectively. This hierarchy is respected in the subsequent back-field experiment (Figure 2), with coercive field being defined only for CB22, at 7.5 T. After a back-field of 9 T, the application of a direct field of 9.3 T does not recover the initial state, due to irreversibility of the demagnetization process. The coercivity appears to increase with T_B and crystallinity (Table 1). RT IRM at 34 T ranges from 8 to 20 mAm^2kg^{-1} and decreases with increasing coercivity. Subsequently GT and 39/80 samples were exposed to larger pulsed fields from 39 to 57 T. Accidentally, this field was applied in the opposite direction of the 34 T field. The fact that IRM up to 57 T remains below the value reached at 34 T, while increasing the field, indicates that a back field of 57 T is not sufficient to reset the 34 T IRM and thus to saturate IRM. The goethite bearing limestone RD (Figure 1b) exhibits a softer behavior than the pure goethite samples (half acquisition field of 3 T) but saturation seems to be reached only around 20 T. The IRM decrease (in both coils) above 20 T is puzzling and could be an effect of relaxation induced by the field pulse.

[6] The RR sample is saturated within 5% at 5 T, and within 1% at 8 T. This is confirmed by the back-field experiment (Figure 2). Such a saturation may be typical for the weak ferromagnetism of single domain hematite. The constant IRM above 8 T confirms the reliability of our

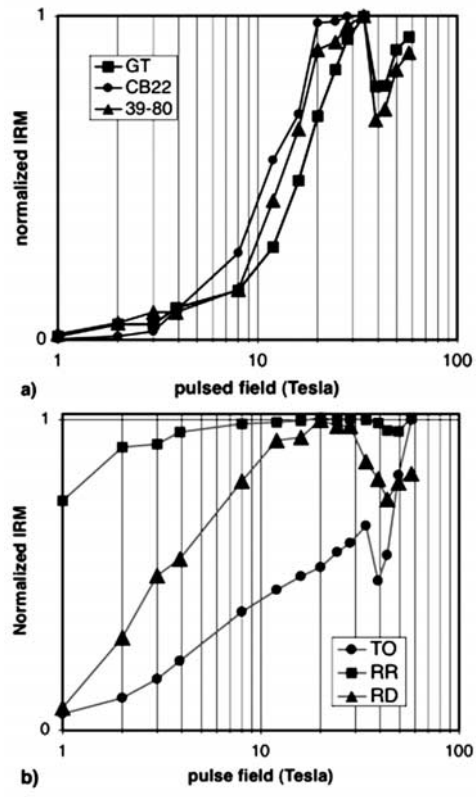

Figure 1. RT IRM acquisition curves up to 57 T normalized to maximum value. (a) Goethite powders, note that CB22 curve is limited to 34 T; (b) rock samples RD, RR and TO. Anomalous decrease in between 34 and 39 T is due to field reversal between the two coils used.

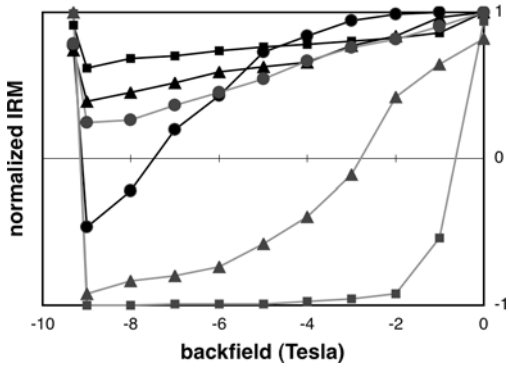

Figure 2. Back field IRM curves after applying a positive 57 T field, normalized to maximum value. Goethite and rock samples as black and gray lines, respectively (same symbols as in Figure 1). Negative fields from −1 to −9T are applied, while the last value (9.3 T) is positive but plotted as negative for a convenient representation. Significant relaxation between acquisition and back-field experiment occurred only for RD.

IRM acquisition and measurement (despite the change of magnet and field polarity in between 34 and 39 T), although more noise appears in the 50 T zone, possibly due to vibrations in the coil. On the other hand the TO sample, after an initial rapid increase (like RR), exhibits a slower linear increase from 10 to 34 T, with no sign of saturation up to 57 T. Contrary to the goethite curves, it seems that the 34 T IRM has been reset by back field around 50 T. For these rock samples the concentration of goethite or hematite cannot be precisely estimated. A lower limit for the maximum IRM (per unit mass of Fe_2O_3), based on assigning all iron to these minerals, is 33, 204 and 92 mAm^2kg^{-1} for RD, RR and TO, respectively.

5. Discussion and Conclusions

[7] Defect moment along the antiferromagnetic axis is due to unbalance between the two antiferromagnetic sublattices. For the goethite powders the coercivity clearly increases with increasing crystallinity/crystallite size and maximum T_B. Maximum IRM decreases with increasing crystallinity. However, is it still quite large for GT large crystals, and we do not know if saturation IRM, if achievable, would not be independent of crystallinity. This does not support the origin of unbalance linked to odd number of iron atoms or surface effects in a nanocrystal [*Néel*, 1962], like recently exemplified on ferritin [*Gilles et al.*, 2002]. Remanence origin cannot be either assigned to the presence of substituted non-magnetic ions, like it is invoked for Al-goethites [*Liu et al.*, 2004].

[8] What is the microscopic process by which IRM is acquired in these systems? As already discussed by *Rochette and Fillion* [1989], the saturation remanence (extrapolated at 0 K) corresponds to at most 1% of imbalance. The corresponding net torque of applied field on the total magnetization is thus negligible with respect to the magnetocrystalline anisotropy. A coherent rotation of both sublattices to align the larger M_s sublattice toward the applied field is therefore excluded. Overcoming the exchange anisotropy to rotate both sublattices near the applied field and let the smaller one revert to opposite direction when the field ramps back to zero is also unrealistic. Room temperature antiferromagnetic susceptibility implies a field of the order of 10^3 T to reach full ferromagnetic saturation (see also Figure 3). The presence of a spin-flop transition decreases somehow this value and could interfere with remanence acquisition. Based on induced magnetization measurement up to 40 T at 4.2 K (Figure 3), we observed on GT sample that the spin-flop transition field (B_t) is about 20 T, confirming the results of *Coey et al.* [1995]. To predict the B_t value at RT one can use the simple law [*Kanamori*, 1963]: $B_t^2 \approx (\chi_{perp} - \chi_{//})^{-1}$. Using the published susceptibility difference versus T values [*Coey et al.*, 1995; *Özdemir and Dunlop*, 1996] one gets a transition field at RT of the order of 40 T. However, if the spin-flop transition was playing a role in the remanence acquisition one would expect a discontinuity in the acquisition curve near B_t, instead of the regular IRM increase (Figure 1).

[9] We interpret our results on the basis of the field-induced diffusion hypothesis [*Rochette and Fillion*, 1989]. Defects responsible for the sublattices imbalance would be pushed into the adequately oriented sublattice by the local magnetic field. The fact that a 57 T back-field is not able to fully erase the remanence acquired in a 34 T field is simply accounted for in this model. The local energy barrier that a defect overcomes to leave its initial position and jump onto the opposite sublattice is in fact independent (thus possibly much lower) from the energy barrier of the backward jump. The actual nature of the defects involved, such as vacancies and Fe^{2+} linked to the replacement of OH^- by H_2O [*Rochette and Fillion*, 1989; *Coey et al.*, 1995] remains to be determined, but they are clearly not linked to substitution of iron by other elements in the case of our pure goethites. Electron-exchange among a Fe^{II}/Fe^{III} pair, or proton exchange between OH^- and H_2O may be in the right energy range for field-induced diffusion. In the case of the non-saturated Mn-bearing hematite of TO sample, a similar model could be invoked, using e.g. different oxidation states of Mn. This hematite, formed at low temperature on the

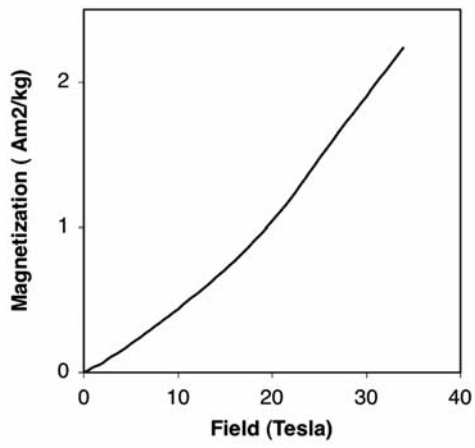

Figure 3. Induced magnetization measured at 4.2 K in the LNCMP pulse system on GT unoriented massive sample. Spin-flop transition corresponds to the slope change around 20 T; see *Coey et al.* [1995] for details on such curves.

ocean floor, is also likely hydrated and poorly crystalline. Scanning electron microscopy indicates for most TO oxyde grains a size of <1 μm, preventing direct confirmation of Mn substitution.

[10] The extreme remanent coercivities evidenced here imply that standard rock magnetic techniques are practically blind to such minerals: the remanence acquired in 3 T is only 2 to 10% of the 57 T remanence of TO hematite and of the pure goethites. The resulting gross underestimation of the magnetic contribution of these minerals challenges rock magneticists to design alternative techniques to probe these essential minerals in supergene environments.

[11] **Acknowledgments.** M. Dekkers and an anonymous reviewer are thanked for their constructive comments. The characterization of synthetic goethites was funded by the Spanish Ministerio de Ciencia y Tecnología, Project AGL2003-01510, while the Pulsed Field facility is funded by EuroMagNET, fP6-I3 n° 506239. We are deeply indebted to R. Trindade (now at IAG San Paolo) for the initial idea of this project.

References

Chevrier, V., P. Rochette, P. E. Mathé, and O. Grauby (2004), Weathering of iron rich phases in simulated Martian atmospheres, *Geology*, *32*, 1033–1036.

Coey, J. M. D., et al. (1995), Spin flop in goethite, *J. Phys. Condens. Matter*, *7*, 759–768.

Dekkers, M. J. (1989), Magnetic properties of natural goethite: 1. Grain size dependence of some low and high field related rock magnetic parameters measured at room temperature, *Geophys. J.*, *97*, 323–340.

Dekkers, M., and P. Rochette (1992), Magnetic properties of CRM in synthetic and natural goethite: Prospect for a NRM/TRM ratio paleomagnetic stability test?, *J. Geophys. Res.*, *97*, 17,291–17,307.

Dunlop, D. J. (1971), Magnetic properties of fine-particle hematite, *Ann. Geophys.*, *27*, 269–293.

France, D. E., and F. Oldfield (2000), Identifying goethite and haematite from rock magnetic measurements of soils and sediments, *J. Geophys. Res.*, *105*, 2781–2795.

Gilles, C., P. Bonville, H. Rakoto, J. M. Broto, K. K. W. Wong, and S. Mann (2002), Magnetic hysteresis and superantiferromagnetism in ferritin nanoparticles, *J. Magn. Magn. Mater.*, *241*, 430–440.

Kanamori, J. (1963), Anisotropy and magnetostriction of ferromagnetic and antiferromagnetic materials, in *Magnetism*, vol. 1, p. 127–203, edited by G. T. Rado and H. Suhl, Elsevier, New York.

Klug, H. P., and L. E. Alexander (1974), *X-ray Diffraction Procedures for Polycrystalline and Amorphous Materials*, 2nd ed., Wiley-Interscience, Hoboken, N. J.

Liu, Q., J. Torrent, Y. Yu, and C. Deng (2004), Mechanism of the parasitic remanence of aluminous goethite [α(Fe, Al)OOH], *J. Geophys. Res.*, *109*, B12106, doi:10.1029/2004JB003352.

Maher, B. A., V. V. Karloukovski, and T. J. Mutch (2004), High-field remanence properties of synthetic and natural submicrometre haematites and goethites: Significance for environmental contexts, *Earth Planet. Sci. Lett.*, *226*, 491–505.

Néel, L. (1962), Propriétés magnétiques des grains fins antiferromagnétiques: Superparamagnetisme et superantiferromagnétisme, *J. Phys. Soc. Jpn.*, *17*, *Suppl. B-1*, 4676–4684.

Özdemir, Ö., and D. J. Dunlop (1996), Thermoremanence and Néel temperature of goethite, *Geophys. Res. Lett.*, *23*, 921–924.

Rochette, P., and G. Fillion (1989), Field and temperature behavior of remanence in synthetic goethite: Paleomagnetic implications, *Geophys. Res. Lett.*, *16*, 851–854.

Schwertmann, U., and R. M. Taylor (1989), Iron oxydes, in *Minerals in Soil Environments*, 2nd ed., edited by J. B. Dixon and S. B. Weed, Soil Sci. Soc. of Am., Madison, Wis.

Thomas, V., J. P. Pozzi, and A. Nicolas (1988), Paleomagnetic results from Oman ophiolites related to their emplacement, *Tectonophysics*, *151*, 297–321.

Torrent, J., U. Schwertmann, and V. Barron (1987), The reductive dissolution of synthetic goethite and hematite in dithionite, *Clay Miner.*, *22*, 329–337.

Torrent, J., V. Barron, and U. Schwertmann (1990), Phosphate adsorption and desorption by goethite of different crystal morphologies, *Soil Sci. Soc. Am. J.*, *54*, 1007–1012.

Van San, E., E. De Grave, and R. E. Vandenberghe (2004), Field-induced spin transitions in hematite powders as observed from Mössbauer spectroscopy, *J. Magn. Magn. Mater.*, *269*, 54–60.

Vlag, P., D. Vandamme, P. Rochette, and K. Spinelli (1997), Paleomagnetism in the Esterel rocks: A revisit 22 years after the thesis of H. Zijderveld, *Geol. Mijnbouw*, *76*, 21–33.

Walden, J., K. H. White, S. H. Kilcoyne, and P. M. Bentley (2000), Analyses of iron oxide assemblages within Namib dune sediments using high field remanence measurements (9 T) and Mössbauer analysis, *J. Quat. Sci.*, *15*, 185–195.

J.-L. Bouchez and L. Esteban, Laboratoire des Mécanismes de Transferts en Géologie, UMR5653, UPS-CNRS, F-31400 Toulouse, France.

Q. Liu, Institute of Geophysics and Planetary Physics, University of California, Santa Cruz, Santa Cruz, CA 95064, USA.

P. E. Mathé and P. Rochette, CEREGE, UMR6635 UPCAM-CNRS, BP80, F-13545 Aix en Provence Cedex 4, France. (rochette@cerege.fr)

H. Rakoto, Laboratoire National des Champs Magnétiques Pulsés, UMR5147, UPS-CNRS-INSA, F-31400 Toulouse, France.

J. Torrent, Departamento de Ciencias y Recursos Agrícolas y Forestales, Universidad de Córdoba, E-14071 Córdoba, Spain.